Bayesian Information Engine that Optimally Exploits Noisy Measurements

Tushar K. Saha[ID],[*] Joseph N. E. Lucero[ID],[§] Jannik Ehrich[ID], David A. Sivak[ID],[‡] and John Bechhoefer[ID][†]

Department of Physics, Simon Fraser University, Burnaby, British Columbia V5A 1S6, Canada

We have experimentally realized an information engine consisting of an optically trapped, heavy bead in water. The device raises the trap center after a favorable "up" thermal fluctuation, thereby increasing the bead's average gravitational potential energy. In the presence of measurement noise, poor feedback decisions degrade its performance; below a critical signal-to-noise ratio, the engine shows a phase transition and cannot store any gravitational energy. However, using Bayesian estimates of the bead's position to make feedback decisions can extract gravitational energy at all measurement noise strengths and has maximum performance benefit at the critical signal-to-noise ratio.

Information engines are a new class of engine that use information as fuel to convert heat from a thermal bath into useful energy. They exploit knowledge of thermal fluctuations to apply feedback and extract energy from the thermal bath, while paying costs required by the second law of thermodynamics to process that information [1]. In the past decade, information engines have been realized in a wide range of physical systems [2–8]. For practical application, it is important to understand how to maximize the engine's output [9,10] and efficiency [10–13]. In addition to straightforward measures of performance such as speed of operation or power imparted to a load, there are also more subtle ones such as the ability to maximize information transmission [14,15].

One obstacle that degrades the output of an information engine is inaccurate information about the system that arises from measurement noise. Since information engines respond to measurements of thermal fluctuations, measurement noise can lead to wrong feedback decisions. Feedback actions chosen based on inaccurate measurements reduce the work extracted from the surrounding thermal bath and can even, at high noise levels, lead to a net heating of the thermal bath [16].

Previous efforts to account for noisy measurements in information engines have all used "naive" feedback algorithms based directly on the most recent noisy measurement [16,17]. Here, we show that such information engines, with unidirectional ratchets, have a phase transition between working and nonworking regimes: Below a critical level of signal-to-noise ratio for measurements of the engine state, a "pure" information engine—one that requires no work input beyond that needed to run the measurement and control apparatus—is not possible.

Although previous studies noted the degradation of performance due to measurement noise, they did not attempt to alter the feedback algorithm to compensate. Yet theoretical studies have indicated that incorporating the information contained in past measurements via optimal feedback control could greatly improve the performance of an information engine [17–20]. Indeed, experiments in other areas of physics have used feedback that incorporates Bayesian estimators to demonstrate spectacular results, even in the presence of high measurement noise; significant achievements include trapping a single fluorescent dye molecule that is freely diffusing in water [21] and cooling a nanoparticle to the quantum regime of dynamics [22,23].

In this Letter, we present an experimental realization of an optimal Bayesian information engine that retains the relevant memory of all past measurements in a single summary statistic. Using the extra information from past measurements and correctly compensating for delays in the feedback loop via predictive estimates, we extract and store significant amounts of energy, even in the presence of high measurement noise.

Our implementation of the Bayesian filter uses the optimal affine feedback control algorithm [24], at optimal experimental parameters [10], to maximize the engine's rate of gravitational-energy storage. The relevant information from past observations is used to minimize the uncertainty in the bead's position. This Bayesian information engine extracts energy even at low signal-to-noise ratio (SNR), avoiding the phase transition in the naive information engine that leads to zero output. Under any conditions, this engine extracts at least as much work as the naive engine and reaches the maximal output power possible for Gaussian information engines [25] subject to an affine feedback rule.

Experimental setup.—Our information engine consists of a 4-μm heavy bead trapped in a horizontally aligned optical trap. Because of the surrounding heat bath, the bead's position fluctuates about an equilibrium average. The heavy bead is also subject to gravity. The bead's position is measured with a sampling time $t_s = 20$ μs using the scattered light from a detection laser.
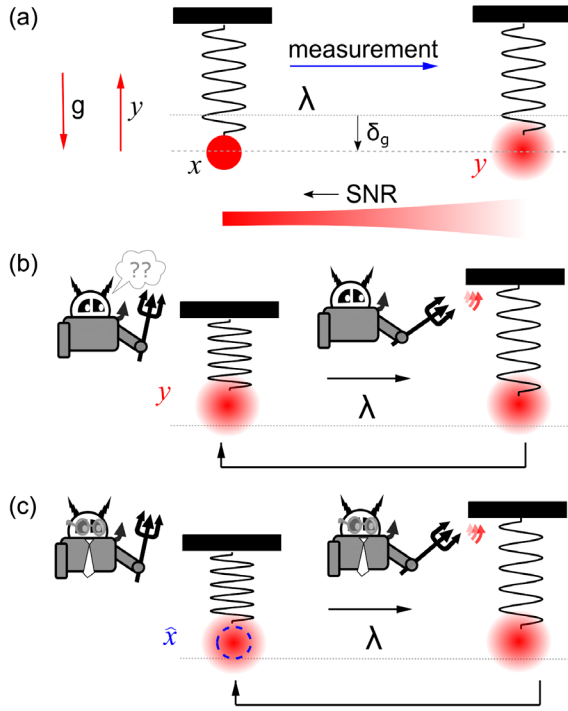
FIG. 1. Schematic information engine. (a) Noisy detector measures position y of the bead, actually located at x. Ratchet based on either (b) noisy position measurement y or (c) Bayesian position estimate $\hat{x}$ (blue dashed circle).

In the operation of the engine, an observed "up" fluctuation increases the bead's gravitational potential energy and can be captured ("rectified") by a quick feedback response that shifts up the trap position. The response takes place after a one-time-step delay $t_d = t_s = 20\ \mu$s, with the shift chosen so that the trap does zero work on the bead. For this "pure" information engine, the work to run the motor is associated only with the measuring device and feedback controller, not the engine itself.

The optically trapped bead can be modeled by a spring-mass system [Fig. 1(a)]. The true position of the bead is estimated from a noisy measurement y. Measurement noise is increased by reducing the intensity of the detection laser beam.

Figure 1(b) shows a "naive" information engine that directly uses a noisy measurement y to apply feedback. By contrast, the "Bayesian" information engine bases its feedback on the best estimate $\hat{x}$ of the bead's position [Fig. 1(c)]. The bead's position is estimated using a Bayesian filter that explicitly models the measurement noise and feedback delay [26].

The information engine can extract energy at high measurement noise because feedback decisions based on filtered estimates of the bead's position are more likely to ratchet to a "true" upward fluctuation rather than to measurement noise.

Equations of motion.—The dynamics of the optically trapped bead obey an overdamped Langevin equation,

$$\gamma\dot{x} = -\kappa[x(t) - \lambda(t)] - mg + \sqrt{2k_B T\gamma}\xi(t), \qquad (1)$$

where $x(t)$ is the position at time t of a bead of diameter d and effective (buoyant) mass m in a trap of stiffness κ and center $\lambda(t)$. The friction coefficient is γ, and $\xi(t)$ is a Gaussian random variable with zero mean and covariance $\langle\xi(t)\xi(s)\rangle = \delta(t - s)$. We denote time derivatives by overdots. Scaling all lengths by the equilibrium position standard deviation $\sigma \equiv \sqrt{k_B T/\kappa}$ and times by the bead relaxation time $\tau_r = \gamma/\kappa$ gives the nondimensionalized Langevin equation

$$\dot{x}(t) = -[x(t) - \lambda(t)] - \delta_g + \sqrt{2}\xi(t) \qquad (2)$$

for scaled effective mass $\delta_g \equiv mg/(\kappa\sigma)$.

Integrating Eq. (2) between measurements from t to $t + t_s$ gives the discrete dynamics

$$x_{k+1} = x_k e^{-t_s} + (1 - e^{-t_s})(\lambda_k - \delta_g) + \sigma_{t_s}\xi_k \qquad (3)$$

for $x_k \equiv x(kt_s)$ and $\lambda_k \equiv \lambda(kt_s)$. The variance $\sigma_{t_s}^2 \equiv 1 - e^{-2t_s}$ of thermal force fluctuations depends on the sampling interval t_s, and ξ_k is a Gaussian random variable with zero mean and covariance $\langle\xi_k\xi_n\rangle = \delta_{kn}$.

The effect of measurement noise is modeled by a measurement variable y_k that is the sum of the bead's true position and additive white Gaussian noise,

$$y_k = x_k + \sigma_m\nu_k, \qquad (4)$$

with ν_k a Gaussian random variable with zero mean and covariance $\langle\nu_k\nu_n\rangle = \delta_{kn}$. We also assume that the thermal noise affecting the bead's position is independent of the measurement noise: $\langle\xi_k\nu_n\rangle = 0$, for all k and n.

The trap position λ_k is updated at each time step using a "ratcheting rule,"

$$\lambda_{k+1} = \lambda_k + \Theta(z_k - \lambda_k)[\alpha\ (z_k - \lambda_k)], \qquad (5)$$

where $\Theta(\cdot)$ denotes the Heaviside function, α the scalar feedback gain, and $z_k \in \{y_k, \hat{x}_{k+1}\}$ the estimate of the bead's position (using either the naive measurement y_k or the Bayesian estimate $\hat{x}_{k+1}$). Because of delays, both the naive and Bayesian estimates of position use information from y_k but not y_{k+1}; however, the Bayesian estimate also implicitly incorporates past information $\{y_{k-1}, y_{k-2}, \ldots\}$ and uses the deterministic component of system dynamics to predict y_{k+1} (see Eq. (6) below).

Estimating the bead position.—Since the actual bead position x fluctuates on a scale σ and the measurement noise fluctuates on a scale σ_m, it is convenient to define a signal-to-noise ratio SNR $\equiv \sigma/\sigma_m$ [27]. In the first "naive" approach to designing feedback based on noisy measurements, the feedback rule, Eq. (5), directly uses the measurement y_k to update the trap position λ_{k+1}. Notice

that this method implicitly estimates the position x_{k+1} by y_k. The naive method performs well at high SNR ($\gg 1$) but poorly at low SNR ($\ll 1$), where a unidirectional ratchet (implemented via the Heaviside function) often responds to noise rather than actual bead movements.

In the second "filtering" approach, we improve the estimate of x_{k+1} by using a Fokker-Planck equation to predict the position probability $p(x_{k+1})$ given $p(x_k)$, which is itself calculated from measurements up to y_{k-1}. One then updates (or "corrects") the prediction for time $k+1$ by incorporating the measurement y_k, using Bayes' rule [[28] Sec. III]. For systems evolving according to linear dynamics and subject to Gaussian noise, $p(x_k)$ remains Gaussian for all k (if $p(x_0)$ is initialized as Gaussian, see Supplemental Material [[28] Sec. III]) and can be summarized by update equations for the mean $\hat{x}_k$ and variance. The Bayesian filter is then known as the "predictive Kalman filter," and one finds [compare Eq. (3)] [34]

$$\hat{x}_{k+1} = \underbrace{\hat{x}_k e^{-t_s} + (1-e^{-t_s})(\lambda_k - \delta_g)}_{\text{predict}} + \underbrace{L\,(y_k - \hat{x}_k)}_{\text{correct}}, \qquad (6)$$

where the scalar filter gain L "corrects" the naive prediction using the difference between the previous estimate and actual observation [[29] Ch. 8]. The gain L is chosen to minimize the variance $\langle (x_k - \hat{x}_k)^2 \rangle$ between the true position and its estimate, and the resulting value is a function of the SNR (see Supplemental Material [[28] Sec. IV, Eqs. (S13) and (S14)]). The variance $\langle (x_k - \hat{x}_k)^2 \rangle$ is always less than that of the naive estimator [35] (see Supplemental Material [[28] Sec. V]); it is optimal in that it incorporates all relevant past information contained in the (long) time series $\{y_k, y_{k-1}, \ldots\}$, and no other unbiased estimator—linear or not—has lower variance [36].

Engine thermodynamics.—Given an estimate of the bead's position, we infer the thermodynamic quantities that characterize this engine's performance. The rate at which we extract gravitational energy (i.e., change in bead free energy) during the time interval $[t_k, t_{k+1})$ is [24]

$$\Delta F_{k+1} = \delta_g(\lambda_{k+1} - \lambda_k), \qquad (7)$$

and the time-averaged rate of free-energy change (more informally, the "output power") is $\dot{F} = \tau^{-1} \sum_k \Delta F_k$, where $\tau = N t_s$ is the total duration of an N-step protocol. We estimate the incremental input work (of the trap on the bead) as

$$\Delta W_{k+1} = \frac{1}{2}[(y_{k+1} - \lambda_{k+1})^2 - (y_{k+1} - \lambda_k)^2], \qquad (8)$$

which estimates input work based on the noisy measurement y_k and not on the true position x_k. The Supplemental Material [[28] Sec. VIII] shows that this input-work estimator is unbiased—the work estimator's mean is equal

to the actual average work value—as a result of feedback delay.

Results.—A "pure" information engine has zero input trap power: $\dot{W} = \tau^{-1} \sum_k \Delta W_k = 0$. Let α^* denote the particular value of the feedback gain α for which the trap power is zero. For an "ideal" pure information engine, one with error-free measurements and no feedback delays, the trap work is zero at $\alpha^* = 2$ [10,28]. Physically, this corresponds to translating the trap to a position opposite its minimum, so that the trap energy is unchanged. Feedback delay and measurement noise reduce α^*. For our experimental conditions with delay of one time step and SNR $= 11$, $\dot{W} = 0$ is satisfied at the lower feedback gain $\alpha^* \approx 1.5$ [Figs. 2(a) and 2(b)].

The Bayesian information engine applies feedback based on the filtered predictive estimate of the bead's position. As such, it accounts in its internal model for feedback delays and measurement noise.

Figure 2(a) shows the input trap power, at fixed SNR ($= 11$), as a function of feedback gain α. Despite the delay and finite SNR, the input trap power is zero for feedback gain $\alpha^* = 2$, similar to that of the "ideal" pure information engine. Figure 2(c) illustrates the operation of the Bayesian
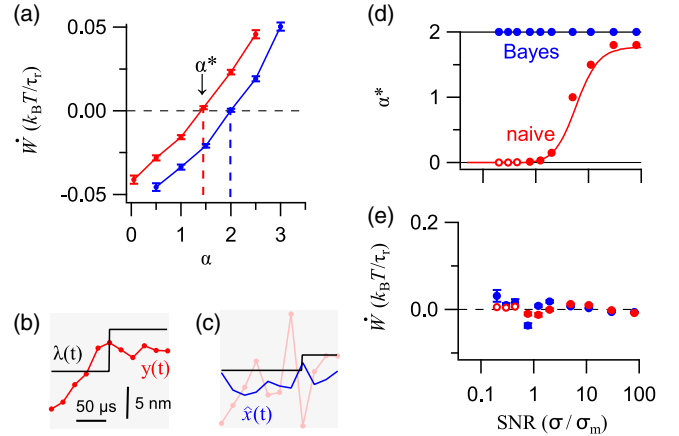
FIG. 2. Tuning the feedback gain α to set trap power $\dot{W} = 0$. (a) Trap power for naive (red) and Bayesian (blue) information engines at fixed SNR $= 11$. (b) Measured bead ($y(t)$, red) and trap ($\lambda(t)$, black) trajectories for the naive information engine at SNR $= 11$. (c) Measured bead ($y(t)$, light red), filtered bead estimate ($\hat{x}(t)$, blue), and trap ($\lambda(t)$, black) trajectories for the Bayesian information engine at SNR $= 2$. (b) and (c) have equal scale bars and satisfy $\dot{W} = 0$. (d) Critical feedback gain α^* and (e) corresponding input trap power, for naive (red) and Bayesian (blue) information engines. Hollow red markers denote SNRs for which $\alpha^* > 0$ could not be found using the procedure outlined in (a). Solid red curve in (d) is from numerical simulation [[28] Sec. VII]. Experiments here and in other figures have sampling frequency $\tau_r/t_s = 41$, trap stiffness $\kappa = 42$ pN/μm, scaled effective mass $\delta_g = 0.8$, diffusion constant $D = 0.12$ μm^2/s, relaxation time $\tau_r = 0.8$ ms, and bead diameter 4 μm. Markers denote experimental means, and error bars the standard errors of the mean.

filter with a trajectory of the Bayesian information engine at lower SNR (= 2). In contrast to the naive information engine, the trap ratchets only when the estimated position (blue) crosses the trap center (black), and not necessarily when the noisy measurement (light red) crosses the trap center.

Next, we investigate how α^* depends on SNR for the naive and Bayesian information engines. For the naive engine, α^* decreases drastically at low SNR [Fig. 2(d)]. For SNR $\lesssim$ SNR$_c$ = 0.7 ± 0.1, where SNR$_c$ denotes the critical vale of the SNR, a nonzero α^* could not be found experimentally using the procedure outlined in Fig. 2(a). The Supplemental Material [[28] Sec. XI] shows that the vanishing of α^* corresponds to a kind of phase transition between a regime where one can set $\dot{F} > 0$ while maintaining $\dot{W} = 0$ and a regime where one cannot.

By contrast, the critical feedback gain α^* remains near 2 for the Bayesian engine [Fig. 2(d)]. The corresponding measured input trap powers for both the naive and Bayesian information engines are close to zero relative to the maximum output power ($\dot{F}_{\max} \approx 0.27 k_B T/\tau_r$) of the engine, at all SNR [Fig. 2(e)].

Taking advantage of predictions in our estimation algorithm thus simplifies the experiments, as it eliminates the need to empirically tune the feedback gain, ensuring that the zero-work condition is always satisfied at $\alpha = 2$. Above, we saw that it also simplifies the work calculations needed to realize a pure information engine, as the value calculated directly from the noisy measurement is an unbiased estimator of the true work.

Finally, Fig. 3(a) compares the performance of the naive and Bayesian information engines, as quantified by the rate of stored gravitational power $\dot{F}$ while keeping $\dot{W} = 0$. Both output powers $\dot{F}$ increase monotonically with SNR and saturate at the same power level at high SNR (> 10).

Although the performance of Bayesian and naive information engines is similar at low and high SNR, there is a striking contrast at intermediate SNR $\lesssim 1$. Indeed, the difference of output powers (Bayesian − naive), normalized by $\dot{F}_{\max}$, significantly exceeds zero for $0.1 \leq$ SNR ≤ 2 and reaches a maximum at SNR $\approx$ SNR$_c$ [Fig. 3(b)].

At high SNR, the Bayesian filter "trusts the observation" and returns an estimate close to the instantaneous measurement, corrected for the expected bias due to the time delay. Since this bias is small for frequent measurements, both engines have similar performance and extract all the favorable thermal fluctuations, saturating at the maximum output power $\dot{F}_{\max} \approx 0.27$. At low SNR, the measurements are so noisy that they exceed the scale of the trap. The Bayesian information engine then extracts negligible power [[28] Sec. IX], while the naive engine extracts zero power. Therefore, at SNR $\gg 1$ and $\ll 1$, the difference of output powers ($\dot{F}_B - \dot{F}_N$) tends to zero. But at intermediate SNR, the effective noise averaging in the Bayesian (Kalman) filter produces more accurate estimates, leading to better feedback decisions and thus improved engine performance.
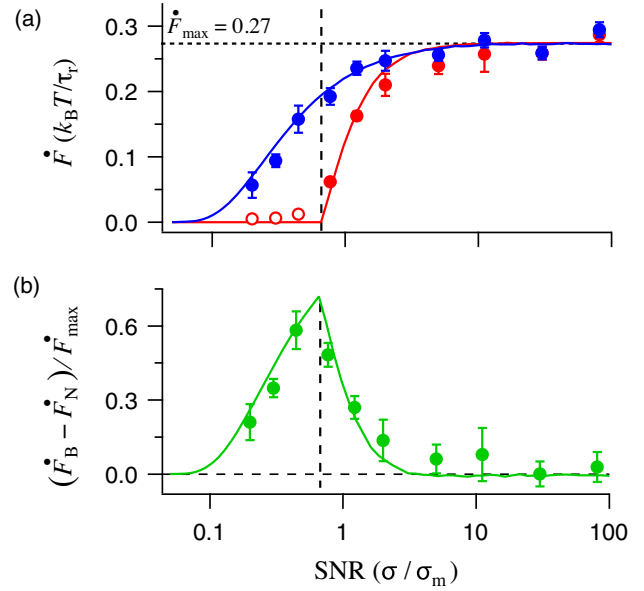
FIG. 3. Performance of the information engines. (a) Output power of naive (red) and Bayesian (blue) information engines as a function of SNR. Hollow red markers denote output power at $\alpha^* = 0$. (b) Difference of output work extraction rates for the Bayesian (B) and naive (N) engines scaled by the maximum rate ($\dot{F}_{\max} = 0.27$). The difference peaks at SNR = SNR$_c \approx 0.7$ (vertical dashed lines). Markers denote experimental means, solid curves the numerical simulations [[28] Sec. VII]. Error bars denote (a) standard error of the mean and (b) propagated standard error of the mean from (a).

To understand why the naive information engine shows a phase transition at a critical signal-to-noise ratio, we numerically solve a self-consistent equation for the SNR at which trap power vanishes. Enforcing the condition that $\alpha^* = 0$ is the unique solution (see Supplemental Material [[28] Sec. X]), we find SNR$_c \approx 0.64$, consistent with both numerical simulations and experiments.

We also find that the phase transition arises from the biased estimate of the bead's position from the noisy measurements. This bias has two origins: the delay due to feedback latency and the failure of the naive measurement to account for the fact that fluctuations above threshold are rare while noise fluctuations of either sign are equally likely. Because fluctuations up to the threshold are rare, the bead is usually below the observed value whenever an apparent threshold crossing is observed.

By contrast, a phase transition does *not* occur for the Bayesian information engine. The Bayesian filter gives an unbiased prediction of the bead's position, accounting for both feedback delay and the "prior" associated with observations near the threshold. As a result, the bead is equally likely to be on either side of the predicted position, allowing one to tune for zero trap power and extract at least some power at *any* SNR value (see Supplemental Material [[28] Sec. XII]).

Conclusion.—Information engines that decide whether to ratchet using single noisy measurements have a phase transition at a critical signal-to-noise ratio SNR_c and cannot function for $SNR < SNR_c$. By contrast, if its feedback uses a Bayesian estimate of bead position that incorporates prior measurements, an information engine can operate at *all* values of SNR. The maximum performance benefit over the naive engine occurs at the critical value SNR_c.

The ability to increase the performance of an information engine at low SNR is important for experimental investigations of motor mechanisms that use fluorescent probes [37]. In such applications, lower light intensities for monitoring fluorescent probes reduce photobleaching and allow longer measurements of motor behavior.

In addition, using a filtering algorithm to reduce the required accuracy of information while maintaining a given performance may decrease the thermodynamic costs of processing position measurements. Generally, a lower measurement accuracy reduces the minimum thermodynamic (Landauer) costs of running the controller [16,38]. However, keeping a memory of past observations should increase those costs, as these costs are related to the mutual information the memory stores about the particle position. Storing more measurements results in more information and hence greater costs. In particular, the Bayesian filter uses recursive update relations to implicitly incorporate information from all past measurements. Alternative filters using a finite number of measurements to make an unbiased position estimate would use less information but lead to engines with lower outputs. Further work is needed to compare the efficiency of a feedback strategy that incorporates a memory of past measurements with one based purely on the most recent measurement. Such studies could evaluate the potential performance trade-offs encountered when varying the measurement accuracy.

[*]Corresponding author.
tushars@sfu.ca
[†]Corresponding author.
johnb@sfu.ca
[‡]Corresponding author.
dsivak@sfu.ca
[§]Also at Department of Chemistry, Stanford University, Stanford, California 94305, USA.

[1] J. M. Parrondo, J. M. Horowitz, and T. Sagawa, Thermodynamics of information, Nat. Phys. **11**, 131 (2015).

[2] S. Toyabe, T. Sagawa, M. Ueda, E. Muneyuki, and M. Sano, Experimental demonstration of information-to-energy conversion and validation of the generalized Jarzynski equality, Nat. Phys. **6**, 988 (2010).

[3] P. A. Camati, J. P. S. Peterson, T. B. Batalhão, K. Micadei, A. M. Souza, R. S. Sarthour, I. S. Oliveira, and R. M. Serra, Experimental Rectification of Entropy Production by Maxwell's Demon in a Quantum System, Phys. Rev. Lett. **117**, 240502 (2016).

[4] J. V. Koski, A. Kutvonen, I. M. Khaymovich, T. Ala-Nissila, and J. P. Pekola, On-Chip Maxwell's Demon as an Information-Powered Refrigerator, Phys. Rev. Lett. **115**, 260602 (2015).

[5] K. Chida, S. Desai, K. Nishiguchi, and A. Fujiwara, Power generator driven by Maxwell's demon, Nat. Commun. **8**, 15310 (2017).

[6] A. Kumar, T.-Y. Wu, F. Giraldo, and D. S. Weiss, Sorting ultracold atoms in a three-dimensional optical lattice in a realization of Maxwell's demon, Nature (London) **561**, 83 (2018).

[7] J. J. Thorn, E. A. Schoene, T. Li, and D. A. Steck, Experimental Realization of an Optical One-Way Barrier for Neutral Atoms, Phys. Rev. Lett. **100**, 240407 (2008).

[8] M. D. Vidrighin, O. Dahlsten, M. Barbieri, M. S. Kim, V. Vedral, and I. A. Walmsley, Photonic Maxwell's Demon, Phys. Rev. Lett. **116**, 050401 (2016).

[9] T. K. Saha and J. Bechhoefer, Trajectory control using an information engine, in *Optical Trapping and Optical Micromanipulation XVIII* (International Society for Optics and Photonics, Bellingham, WA, 2021), Vol. 11798, p. 117980L, 10.1117/12.2593992.

[10] T. K. Saha, J. N. E. Lucero, J. Ehrich, D. A. Sivak, and J. Bechhoefer, Maximizing power and velocity of an information engine, Proc. Natl. Acad. Sci. U.S.A. **118** (2021).

[11] G. Paneru, D. Y. Lee, T. Tlusty, and H. K. Pak, Lossless Brownian Information Engine, Phys. Rev. Lett. **120**, 020601 (2018).

[12] T. Admon, S. Rahav, and Y. Roichman, Experimental Realization of an Information Machine with Tunable Temporal Correlations, Phys. Rev. Lett. **121**, 180601 (2018).

[13] M. Ribezzi-Crivellari and F. Ritort, Large work extraction and the Landauer limit in a continuous Maxwell demon, Nat. Phys. **15**, 660 (2019).

[14] Y. Tang and A. Hoffmann, Quantifying information of intracellular signaling: Progress with machine learning, Rep. Prog. Phys. **85**, 086602 (2022).

[15] F. Schaper, T. Jetka, and A. Dittrich, Decoding cellular communication: An information theoretic perspective on cytokine and endocrine signaling, Curr. Opin. Endocr. Metab. Res. **24**, 100351 (2022).

[16] G. Paneru, S. Dutta, T. Sagawa, T. Tlusty, and H. K. Pak, Efficiency fluctuations and noise induced refrigerator-to-heater transition in information engines, Nat. Commun. **11**, 1012 (2020).

[17] A. Taghvaei, O. M. Miangolarra, R. Fu, Y. Chen, and T. T. Georgiou, On the relation between information and power in

stochastic thermodynamic engines, IEEE Control Syst. Lett. **6,** 434 (2022).

[18] K. Nakamura and T. J. Kobayashi, Connection Between the Bacterial Chemotactic Network and Optimal Filtering, Phys. Rev. Lett. **126,** 128102 (2021).

[19] J. M. Horowitz, T. Sagawa, and J. M. R. Parrondo, Imitating Chemical Motors with Optimal Information Motors, Phys. Rev. Lett. **111,** 010602 (2013).

[20] N. Rupprecht and D. C. Vural, Predictive Maxwell's demons, Phys. Rev. E **102,** 062145 (2020).

[21] A. P. Fields and A. E. Cohen, Electrokinetic trapping at the one nanometer limit, Proc. Natl. Acad. Sci. U.S.A. **108,** 8937 (2011).

[22] L. Magrini, P. Rosenzweig, C. Bach, A. Deutschmann-Olek, S. G. Hofer, S. Hong, N. Kiesel, A. Kugi, and M. Aspelmeyer, Real-time optimal quantum control of mechanical motion at room temperature, Nature (London) **595,** 373 (2021).

[23] G. P. Conangla, F. Ricci, M. T. Cuairan, A. W. Schell, N. Meyer, and R. Quidant, Optimal Feedback Cooling of a Charged Levitated Nanoparticle with Adaptive Control, Phys. Rev. Lett. **122,** 223602 (2019).

[24] J. N. E. Lucero, J. Ehrich, J. Bechhoefer, and D. A. Sivak, Maximal fluctuation exploitation in Gaussian information engines, Phys. Rev. E **104,** 044122 (2021).

[25] Gaussian information engines are a class of information engines where the system—a particle in our case—is subject to both a linear deterministic force and a Gaussian stochastic force, and where measurements of the system state are contaminated by a different, independent, Gaussian white noise. As such, the Markov dynamical propagator that governs the dynamics of the system probability distribution is also Gaussian.

[26] The delay is also termed "feedback latency," which refers explicitly to the sum of delays in the feedback loop, which include contributions from measurements, computations, and output to the actuator (the acousto-optic deflector, which moves the trap center). We use the more familiar informal language in the text.

[27] SNR is often alternately defined as a ratio of signal-to-noise power, σ^2 / σ_m^2.

[28] See Supplemental Material at http://link.aps.org/supplemental/10.1103/PhysRevLett.129.130601 for more discussion of the experimental setup, the Bayesian estimator, and the phase transition, which includes Refs. [10,29–33].

[29] J. Bechhoefer, *Control Theory for Physicists* (Cambridge University Press, Cambridge, England, 2021).

[30] A. Kumar and J. Bechhoefer, Nanoscale virtual potentials using optical tweezers, Appl. Phys. Lett. **113,** 183702 (2018).

[31] K. Berg-Sørensen and H. Flyvbjerg, Power spectrum analysis for optical tweezers, Rev. Sci. Instrum. **75,** 594 (2004).

[32] Q. Wang and W. E. Moerner, An adaptive anti-Brownian electrokinetic trap with real-time information on single-molecule diffusivity and mobility, ACS Nano **7,** 5792 (2011).

[33] K. Sekimoto, *Stochastic Energetics* (Springer, New York, 2010).

[34] Note that the predictive Kalman filter first *predicts* the position of the bead using the same model of deterministic dynamics that is present in the particle's equation of motion. It then *corrects* this prediction using the (noisy) observation.

[35] The Bayesian estimator has lower variance than that of the naive estimator provided that the Kalman gain L has the optimal value given by Eq. (S14). If it had a sufficiently different value, the Bayesian estimator variance could exceed that of the naive estimator.

[36] T. Kailath, A. H. Sayed, and B. Hassibi, *Linear Estimation* (Prentice Hall, Englewood Cliffs, NJ, 2000).

[37] C. Veigel and C. F. Schmidt, Moving into the cell: Single-molecule studies of molecular motors in complex environments, Nat. Rev. Mol. Cell Biol. **12,** 163 (2011).

[38] J. M. Horowitz and H. Sandberg, Second-law-like inequalities with information and their interpretations, New J. Phys. **16,** 125007 (2014).